The effect of annealing on properties of AISI 316L base and weld metals

Vpliv žarjenja na lastnosti osnovnega materiala in vara jekla AISI 316L

Stjepan Kožuh[1], Mirko Gojić[1], Ladislav Kosec[2]

[1]University of Zagreb, Faculty of Metallurgy, Aleja narodnih heroja 3, 44103 Sisak, Croatia; E-mail: kozuh@simet.hr, gojic@simet.hr
[2]University of Ljubljana, Faculty of Natural Sciences and Engineering, Aškerčeva cesta 12, SI-1000 Ljubljana, Slovenia; E-mail: kosec@ntf.uni-lj.si

Received: November 14, 2007 **Accepted:** December 4, 2007

Abstract: Results of mechanical testing and of microstructural analysis of AISI 316L austenitic stainless steel carried out before and after welding and post-weld heat treatment are presented. Steel plates of 15 mm thickness were welded by manual electric arc welding process. Heat treatment consisted of annealing at 600, 700, 800, and 900 °C for two hours, and was followed by cooling in the air. For microstructure examination an optical microscope and a scanning electron microscope were used. The weld metal microstructure demonstrated the presence of austenite, ferrite, and microslag inclusions before annealing, and of sigma phase after annealing. The tensile strength increased and impact energy values decreased with the increasing annealing temperature. Complex Mn-Cr-Si-Ti inclusions in the dimples were observed in the tensile and Charpy tested specimens.

Izvleček: V članku so opisani rezultati preiskav mehanskih lastnosti in analiza mikrostrukture avstentnega jekla AISI 316L pred in po varjenju ter toplotni obdelavi zvarov. 15 mm debele jeklene plošče so bile zvarjene ročno elektro obločno. Zvari so bili žarjeni dve uri na temperaturah 600, 700, 800 in 900 °C ter nato ohlajeni na zraku. Mikrostrukturne raziskave smo opravili z optičnim in vrstičnim elektronskim mikroskopom. V mikrostrukturi vara so značilne sestavine avstenit, ferit in vključki žlindre, po žarjenju pa faza σ. S temperaturo žarjenja raste natezna trdnost, obratno pa se zmanjšuje žilavost varov. Na prelomnih površinah obeh vrst epruvet smo v jamicah žilavega preloma opazili kompleksne nekovinske vključke z glavnimi kovinskimi sestavinami Mn-Cr-Si-Ti.

Key words: stainless steel, austenite, welding, microstructure, mechanical properties, sigma phase

Ključne besede: nerjavno jeklo, avstenit, varjenje, mikrostruktura, mehanske lastnosti, faza σ

Scientific paper

INTRODUCTION

Stainless steels constitute a group of high-alloyed steels based on the Fe-Cr, Fe-Cr-Ni, and Fe-Cr-C systems. To be classified as stainless, the steels must contain a minimum of 11 % chromium, but less than 30 % [1]. Austenitic stainless steels are an important class of stainless materials that have been used widely in a variety of industries and environments. The basic austenitic composition is the familiar 18 % chromium and 8 % nickel alloy. The increased chromium and nickel contents can improve corrosion resistance, and addition of other elements (most commonly molybdenum in AISI 316L) can enhance it further. For stainless steels welding is an important fabrication technique. In general, stainless steels are considered to be weldable materials, but there is a number of rules to be observed to ensure that they are readily fabricated free from defects, and that they perform as expected in their intended service[2]. Almost certainly, welding will bring about a major microstructural alteration in the weld metal and in the heat-affected zone with respect to the base metal. Weld solidification and liquation cracking will depend on the composition of the base and filler metals, and on the level of impurities, particularly of sulphur and phosphorus.

The complexity of the weld metal microstructure is attributable to the mode of solidification and to subsequent solid-state phase transformation. Depending on the alloy composition, austenite may originate in two ways: from a eutectic reaction and partial solid-state transformation of ferrite, or as a result of ferrite decomposition during postsolidification cooling. Austenitic steels may undergo microstructural changes during short- or long-term exposure to high temperature[3]. HEINO et al.[4] reported that during heat treatment of austenitic stainless steels at 600-900 °C, short-time precipitation from austenite (<60 s) was typically associated with the formation of $M_{23}C_6$ carbide. In the case of longer ageing times, other precipitates such as intermetallic phases are formed, which are usually accompanied by dissolution of carbides. The intermetallic precipitations are of great interest not only because they exert influence on the mechanical properties but also because of their strong effect on the corrosive properties. There have been many studies into the microstructure and the precipitation behaviour of stainless steels during welding and in exposure to elevated temperatures[5-9].

The two intermetallic phases most commonly found in austenitic stainless steels are sigma phase and χ phase[10]. Sigma phase is an intermetallic compound with a complex tetragonal crystalline structure. Its composition varies fairly widely and is difficult to describe by means of a formula. Thus, according to literature[11] a typical sigma phase composition for the AISI 316L steel type is 44 % Fe - 29 % Cr - 8 % Mo. At room temperature sigma phase is hard, brittle and nonmagnetic. Its promotion elements are molybdenum, silicon, vanadium, tungsten and columbium, whereas carbon, nitrogen and nickel retard sigma formation. Sigma phase is responsible for reduction in toughness at room temperature. Embrittlement, if it occurs, can be removed by dissolving sigma at temperatures above 1000 °C. Rapid cooling is recommended

to avoid brittleness at 475 °C. In contrast to sigma phase, the precipitation of the χ phase in austenitic stainless steels is thermodynamically unstable. With the onset of sigma precipitation, the χ phase vanishes in its favour.

This work is focussed on the effect of post-weld heat treatment of the base and weld metals on their mechanical properties and microstructures. It aims to find out how mechanical properties and impact energy are affected by the sigma phase precipitation, and to determine, by EDX analysis, the sigma phase composition. On the other hand, interpretation of the fracture mechanism can provide valuable evidence for the cause of failure.

Experimental

The austenitic stainless steel in this experiment was AISI 316L. Its chemical composition is given in Table 1. Welding of a steel sheet of 15 mm thickness was carried out by the manual electric arc welding process using solid electrodes 2.5 and 3.25 mm in diameter. Before welding the sheet surfaces were thoroughly cleaned and then brushed. The V-joints were prepared with the Böhler FOX SAS-4A electrodes. Immediately after welding the welded joint was subjected to post-weld heat treatment at 600-900 °C for two hours, and was then cooled in the air.

Tensile testing was carried out in conformity with ASTM standards[12]. It was done with an Instron tensile machine, type 1196, on nonwelded and as-welded specimens at room temperature. Hardness was measured by the Vickers test (HV_{30}). Impact tests were performed on Charpy V-notch specimens (10×10×55 mm) at room temperature. A V-notch of 2 mm depth was machined in the middle of a weld metal sample.

Microstructural analysis of the base and weld metals was carried out by optical microscopy and scanning electron microscopy. Samples for microstructural analysis were subsequently ground, polished and electrolytically etched. To expose austenite boundaries 60 ml HNO_3 and 40 ml water solution was used at 1V DC for 20 s. Sigma phase and ferrite were identified with 56 g KOH in 100 ml water at 2V DC for 10 s.

Fractographic analysis was carried out after both tensile and impact energy testing. Surface fractures were tested with a SEM JEOL JSM-5610 Model 500 Analyser operating at 20 kV and equipped with EDAX and XRF systems. The delta ferrite number in the base and weld metals was determined by means of a ferritoscope. The method takes advantage of the fact that ferrite is magnetic and austenite is not.

Table 1. Chemical composition of the base (BM) and weld metals (WM) [wt.%]
Tabela 1. Kemična sestava osnovnega materiala (BM) in vara (WM) [m.%]

	C	Mn	Si	Cu	V	Mo	Al	Cr	Ni	W	Ti	Nb
BM	0.026	1.49	0.45	0.35	0.060	2.04	0.008	16.75	10.80	0.066	0.081	0.016
WM	0.024	0.85	0.74	0.11	0.074	2.44	0.004	19.15	10.86	0.048	0.009	0.289

Table 2. Mechanical properties of the base and weld metals before post-weld heat treatment
Tabela 2. Mehanske lastnosti osnovnega materiala in vara pred toplotno obdelavo

	Yield strength, [N/mm²]	Tensile strength, [N/mm²]	Reduction of area, [%]	Impact energy, [J]
Base metal	270.7	606.3	75.1	238.3
Weld metal	-	732.7	52.1	83.3

RESULTS AND DISCUSSION

Table 2 and Figure 1 show results of tensile and impact testing of the base and weld metals before annealing and after it. The values are expressed as the means of three measurements. The tensile strength of the weld metal was higher than that of the base metal. The area reduction for the base metal (about 75 %) was higher than for the weld metal (52 %), and decreased with a rise in the annealing temperature. Elevated annealing temperature produced a remarkable drop in impact energy of either metal (Figure 1). The most likely reason for this was the precipitation of the sigma phase particles which improved strength and reduced plasticity and toughness.

Figure 2 shows Vickers hardness distribution and the effect of annealing temperature on the hardness of the base metal, heat-affected zone and weld metal. The weld metal exibited remarkably higher hardness values than the base metal (Table 3). This could be accounted for by the weld metal chromium content of about 19.0 wt.%, which was higher than that of the base metal (Table 1). It is generally believed that the elevated chromium content of the weld metal, along with the presence of niobium, increases steel hardenability[1]. This is in agreement with the results of OHKUBO et al.[13] who investigated the effect of alloying elements on the mechanical properties of austenitic stainless steel. Elevated weld metal hardness could also be due

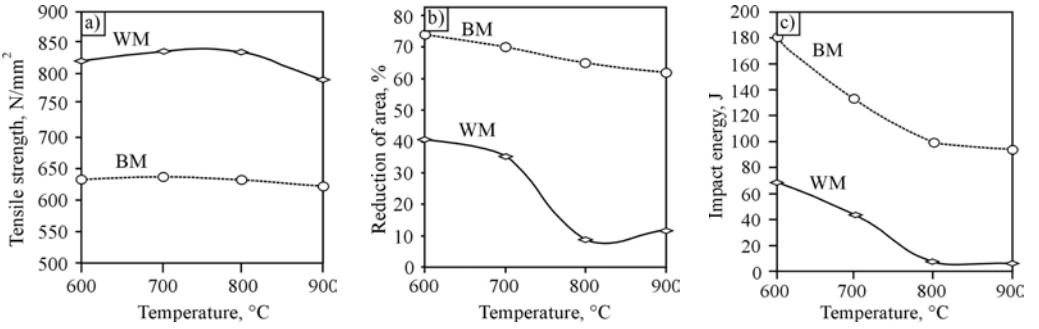

Figure 1. Effect of annealing temperature on tensile strength (a), on area reduction (b), and on impact energy (c) of the base (BM) and weld metals (WM)
Slika 1. Vpliv temperature žarjenja na trdnost (a), kontrakcijo (b) in udarno žilavost (c) osnovnega materiala (BM) in vara (WM)

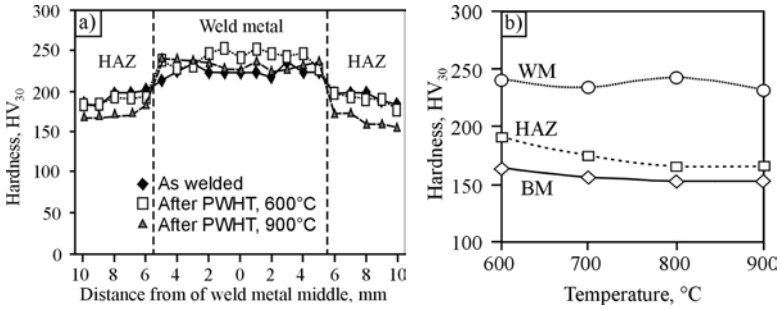

Figure 2. Distribution of Vickers hardness HV_{30} in the welded sections after welding and after post-weld heat treatment (a) and the effect of annealing temperature on hardness (b)

Slika 2. Potek trdote v varu in coni toplotnega vpliva po varjenju in po toplotni obdelavi (a) in učinek toplotne obdelave na trdoto v osnovnih področjih zvara (b)

to heat input during welding, melting and solidification of the area. After annealing, hardness values diminished for the base metal. This could be attributed to a lower stress level and to a change in microstructure.

The microstructure that evolves in a weldment is heterogeneous owing to the temperature gradient associated with the welding process, and the chemical gradient which is generated during that process. As a result of microstructural inhomogeneity gradients in mechanical properties may become noticeable across the weldment.

The microstructure of AISI 316L steel before post-weld heat treatment was austenitic without grain boundary precipitation, as shown in Figures 3 and 4. Ideally, austenitic stainless steels will exibit a single phase that is maintained over a wide temperature range. However, a fully austenitic microstructure is more crack sensitive than the one containing a small amount of ferrite. Figure 3a shows austenitic polygonal grains of AISI 316L stainless steel base metal with a low delta ferrite content. Grain size was G=7.58, and average grain area 679 μm^2 with 1496 grains/unit area. Stringers of delta ferrite can be seen elongated in the rolling direction. The beneficial effect of delta ferrite, which is manifested as decreased susceptibility to hot cracking, stems from its capacity to dissolve harmful impurities such as sulphur, phosphorus, and boron[14].

Table 3. Hardness test results for the base and weld metals before post-weld heat treatment and after it

Tabela 3. Trdote v osnovnem materialu in varu pred in po toplotnih obdelavah zvara

	Hardness, HV_{30}				
	Before annealing	Temperature of annealing [°C]			
		600	700	800	900
Base metal	167.3	164.3	155.6	152.3	153.3
Weld metal	224.2	240.9	233.7	241.5	232.2

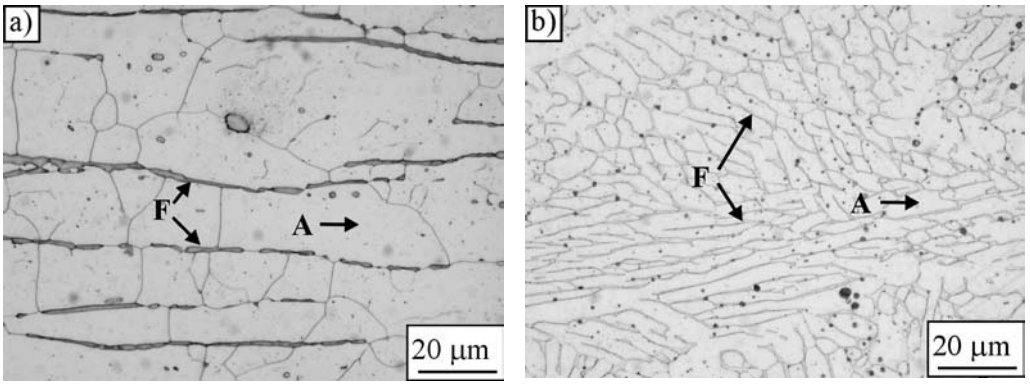

Figure 3. Optical micrograph of AISI 316L stainless steel base metal (a) and weld metal (b) before post-weld heat treatment; A - austenite, F - ferrite
Slika 3. Optično mikroskopska slika mikrostrukture osnovnega materiala (nerjavno jeklo AISI 316L) (a) in vara (b) pred toplotno obdelavo; A - avstenit, F- ferit

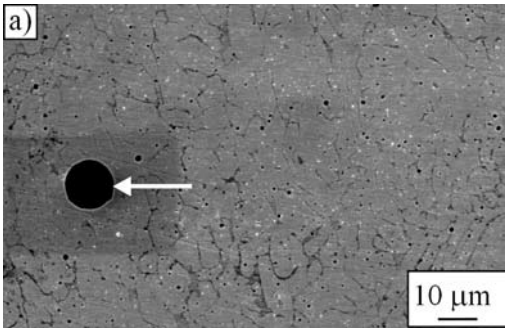

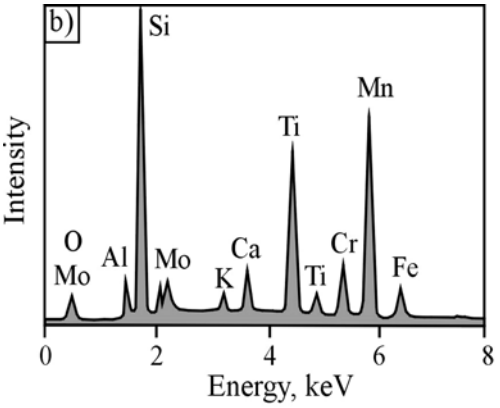

Element	Line	Intensity (c/s)	Concentration (wt.%)
O	K_α	23.20	3.92
Al	K_α	41.33	2.31
Si	K_α	383.71	19.58
K	K_α	30.56	1.50
Ca	K_α	66.37	3.34
Ti	K_α	284.95	18.39
Cr	K_α	95.70	8.39
Mn	K_α	364.57	37.01
Fe	K_α	14.57	1.68
Mo	L_α	30.29	3.01
Other			0.87

Figure 4. SEM micrograph of the weld metal (a) with the corresponding nonmetallic inclusion (b)
Slika 4. Elektronsko mikroskopski (SEM) posnetek mikrostrukture vara (a) s kvalitativno in kvantitativno kemično mikroanalizo nekovinskega vključka (b)

Phase transformations in austenitic stainless steels can be determined with the help of chromium and nickel equivalencies[15]. For the AISI 316L steel base metal in this work, the Cr_{eq}/Ni_{eq} ratio was 1.59, and the final microstructure consisted of austenite and 3.4 % delta ferrite. It is generally held that a 4-8 % delta ferrite content of the base metal is an effective means of offseting a grain boundary weakness that develops in austenite at high temperatures and leads to fissuring. However, high ferrite has been reported to reduce corrosion resistance drastically, and to promote high-temperature embrittlement[16].

In this work the base metal microstructure differed from the microstructure of the weld metal (Figure 3b). The Cr_{eq}/Ni_{eq} ratio was 1.91, and the final weld metal microstructure consisted of austenite and 14.2 % delta ferrite. At room temperature the microstructure of the austenitic stainless steel weld metal is dependent on the solidification behaviour and on subsequent solid-state transformation. Austenitic stainless steels may solidify as primary ferrite or primary austenite i.e. solidification behaviour of the weld metal can be classified into four modes (A, AF, FA, and F). The A and AF solidification modes are associated with primary austenite solidification, whereby austenite is the first phase to form upon solidification. The FA and F solidification types have delta ferrite as the primary phase. The sequence of primary delta ferrite solidification is as follows[17]:

$$L \rightarrow L+\delta \rightarrow L+\delta+\gamma \rightarrow \gamma+\delta \quad (1)$$

According to literature[18],[19] for commercial 300-series stainless steels the weld metal solidification mode for $Cr_{eq}/Ni_{eq} = 1.91$ is FA (FA mode: $1.48 \leq Cr_{eq}/Ni_{eq} \leq 1.95$). If some austenite forms at the end of solidification, it is termed Type FA. This austenite is result of a peritectic-eutectic reaction and can be found at the ferrite solidification boundaries. With this solidification mode, the potential for cracking will be effectively nil. The presence of intermetallic sigma phase in the weld metal before post-weld heat treatment was not observed (Figure 4). In the weld metal microstructure sporadic complex Fe-Mn-Si-Ti-Cr inclusions were present. During tensile testing, the impurity particles fractured or broke off.

The weld metal microstructure after post-weld heat treatment consisted of austenite grains with sigma phase particles (Figures 5 and 6). Figures 5a and 6a show the microstructure of the precipitated sigma phase, and Figures 5b and 6b the compositions of the precipitated phases as determined by EDX using a SEM JEOL JSM-5610. It is well known that in low-carbon austenitic stainless steel the grain boundary precipitation involves mainly nitrides, carbides and intermetallic phases. Thus, after the solution annealing treatments at different temperatures, the intermetallic sigma phase initially precipitates along the delta ferrite/austenite interface. With increase in the annealing temperature the sigma phase precipitation intensifies. Its original composition is iron and chromium based. Sigma phase has a tetragonal crystallographic structure with an elemental cell of 32 atoms and five crystallographically different atom sites[20]. As seen in Figure 5a the sigma phase particles could be observed at the ferrite/austenite grain boundaries. The sigma phase morphology was usually

equiaxed. It changed with the precipitation temperature. At lower precipitation temperatures (600 and 700 °C), a coral-like sigma phase structure could be found. At higher temperatures (800 and 900 °C) the sigma phase was larger and more compact. The presence of sigma precipitates in microstructure can lead to degradation of corrosion resistance, localized stresses at the interfaces between the sigma particles and the matrix, altered crack propagation behaviour, and reduced fracture toughness.

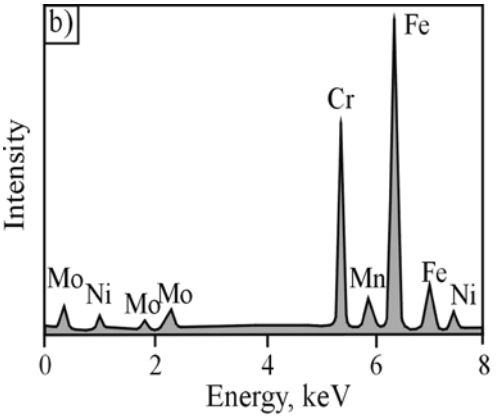

Element	Line	Intensity (c/s)	Concentration (wt.%)
Cr	K_α	395.63	24.37
Mn	K_α	10.29	0.84
Fe	K_α	677.60	67.49
Ni	K_α	36.90	5.42
Mo	L_α	21.78	1.87

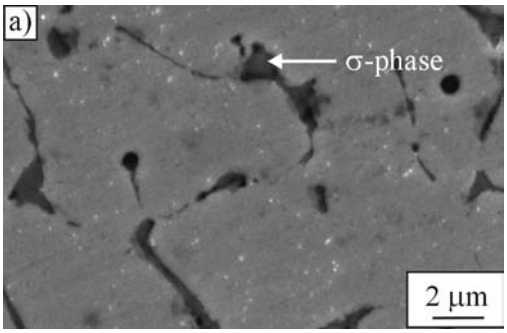

Figure 5. SEM micrograph of AISI 316L steel weld metal (a) with the corresponding EDX spectrum of sigma phase (b) after post-weld heat treatment at 700 °C

Slika 5. Elektronsko mikroskopski (SEM) posnetek mikrostrukture vara jekla AISI 316L (a) s kvalitativno in kvantitativno kemično mikroanalizo delca faze σ (b) po žarjenju na 700 °C

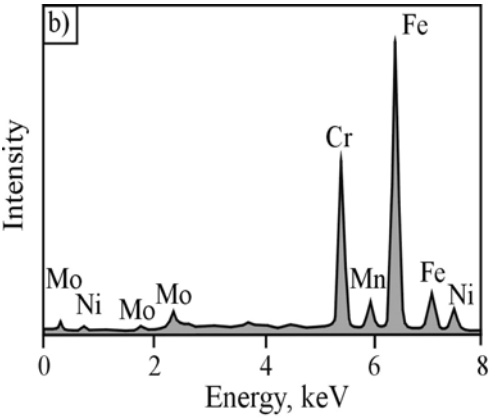

Element	Line	Intensity (c/s)	Concentration (wt.%)
Cr	K_α	400.75	22.72
Mn	K_α	12.73	0.96
Fe	K_α	729.34	66.65
Ni	K_α	55.10	7.45
Mo	L_α	27.79	2.22

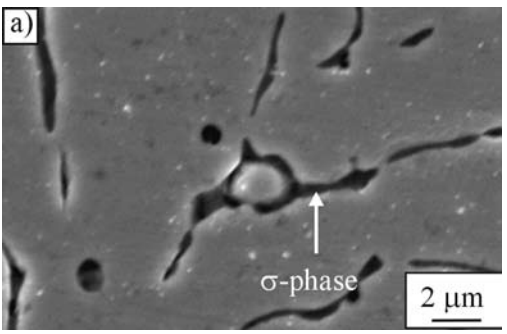

Figure 6. SEM micrograph of AISI 316L steel weld metal (a) with the corresponding EDX spectrum of sigma phase (b) after post-weld heat treatment at 900 °C

Slika 6. Elektronsko mikroskopski (SEM) posnetek mikrostrukture vara jekla AISI 316L (a) s kvalitativno in kvanitativno kemično mikroanalizo mikrostrukturne sestavine faze σ (b) po žarjenju na 900 °C

The EDX analysis showed iron, chromium, and nickel to be dominant sigma phase elements (Figures 5b and 6b). In this work the sigma phase composition was 65-67 % Fe, 22-26 % Cr, 5-7 % Ni, and about 2 % Mo (in wt.). It was slightly different from the typical sigma phase composition of AISI 316 or 316L steels which is 55 % Fe, 29 % Cr, 5 % Ni, and 11 % Mo (in wt.)[21]. As the sigma phase composition tends to vary it is difficult to define it by a formula. The sigma phase precipitation tends to deplete the adjacent chromium matrix. The presence of the chromium depleted zones, which are possible pitting sites, can enhance embrittlement in pitting resistance. After heat treatment the precipitation of the brittle sigma phase produced a considerable drop in impact energy values (Table 3).

The mechanism of sigma phase nucleation is still a matter of controversy and depends on the amount of delta ferrite. The delta ferrite content of the weld metal plays an important role in determining fabrication and service performance of the welded structures. David[22] observed four distinct types of ferrite morphology in stainless steel with a delta ferrite content from 9 to 15 %: vermicular, lacy, acicular, and globular. Variations in ferrite morphology are related to the weld metal composition, ferrite content, and ferrite distribution as a result of thermal cycling during subsequent weld passes. The delta ferrite content of the base and weld metals decreased with the increasing annealing temperature (Table 4). Its transformation was calculated from the values measured before heat treatment and after it. The percentage of delta ferrite decomposition in the weld metal increased from 17.6 % at 600 °C to 96.5 % at 900 °C. It also increased for the base metal, from 23.5 % to 88.2 %. Park et al.[23] investigated fast formation of sigma phase in AISI 304 stainless steel during welding. They suggested that the sigma phase formation could be accelerated by the emergence of delta ferrite at high temperature, and its subsequent decomposition under high strain and recrystallization induced by welding. Kington et al.[7] reported a very rapid sigma phase formation from ferrite in AISI 310 steel at temperatures in excess of 800 °C (complete transformation occurred within 10 minutes at a temperature between 800 and 900 °C). The size, morphology, and distribution of the sigma precipitates and ferrite were sufficiently similar to suggest that the sigma phase had formed by direct ferrite transformation.

Fractographic analysis can describe the fracture process and provide valuable evidence for the cause of failure[14]. In order to determine the fracture mode during tensile and impact energy testing, the failed specimens were examined using a SEM technique. Examination of the fractured specimens demonstrated that the fracture surface was characterized by two fracture modes: a ductile fracture and a cleavage fracture (Figure 7). Dimple morphology dominated on the fracture surface of all samples (Figures 8 and 9). This feature is indicative of a ductile fracture mode. The fracture process is very complex and involves nucleation, growth of micro-voids or cracks, and propagation of these defects. A number of inclusions in small holes were visible on the microfractographs. The EDX analysis demonstrated the presence of complex Mn-Cr-Si-Ti inclusions (Figure 9b).

Table 4. Delta ferrite content of the base and weld metals after post-weld heat treatment [wt.%]
Tabela 4. Delež ferita - δ v osnovnem materialu in varu po žarjenju [m.%]

	Temperature of annealing [°C]	600	700	800	900
Base metal	δ-ferrit, wt.%	2.6	1.2	0.4	0.7
	Decomposition ratio, %	23.5	64.7	88.2	79.4
Weld metal	δ-ferrit, wt.%	11.7	8.0	0.9	0.5
	Decomposition ratio, %	17.6	43.6	93.7	96.5

CONCLUSIONS

Results of investigation into the mechanical properties and microstructure of AISI 316L stainless steel before post-weld heat treatment and after it suggest the following:

- The tensile strength of the weld metal was higher than that of the base metal. The impact energy values and the area reduction decreased drastically with the increasing annealing temperature.
- The hardness test results for the weld metal were remarkably higher than those for the base metal. Comparison of the hardness values measured before post-weld heat treatment and after it showed insignificant variations.
- The base metal consisted of equiaxed austenite grains with some ferrite stringers (3.4 %). The weld metal contained over 14 % of delta ferrite as the result of FA solidification mode during cooling of the welds.
- The delta ferrite content decreased with the increasing annealing temperature. The percentage of delta ferrite decomposition in the weld metal increased from 17.6 % at 600 °C to 96.5 % at 900 °C. It also increased for the base metal, from 23.5 % to 88.2 %.
- Before post-weld heat treatment the weld metal microstructure consisted of austenite and ferrite. Complex microslag inclusions were also present. The EDX analysis showed manganese, silicon, titanium, and chromium to be dominant elements in the inclusions.
- After post-weld heat treatment the presence of sigma phase at the ferrite/austenite boundaries was established by EDX analysis as the result of delta ferrite transformation at elevated temperature. Its composition was 65-67 % Fe, 22-26 % Cr, 5-7 % Ni, and about 2 % Mo. The presence of sigma phase was considered to be adverse to impact energy.
- Two distinct fracture modes were

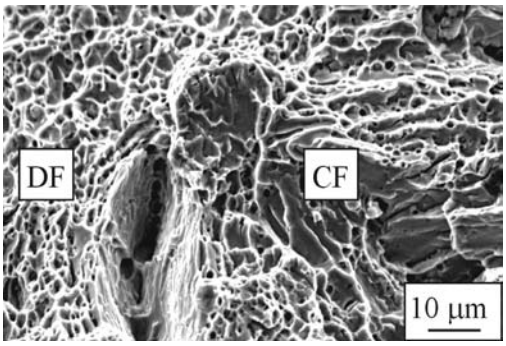

Figure 7. SEM microfractograph of AISI 316L steel weld metal after Charpy impact testing; DF - ductile fracture, CF - cleavage fracture
Slika 7. Mikrofraktografija prelomne površine epruvete za preizkus udarne žilavosti po Charpyju vara jekla AISI 316L; DF duktilni, jamičast prelom; CF - krhki prelom s cepljenjem

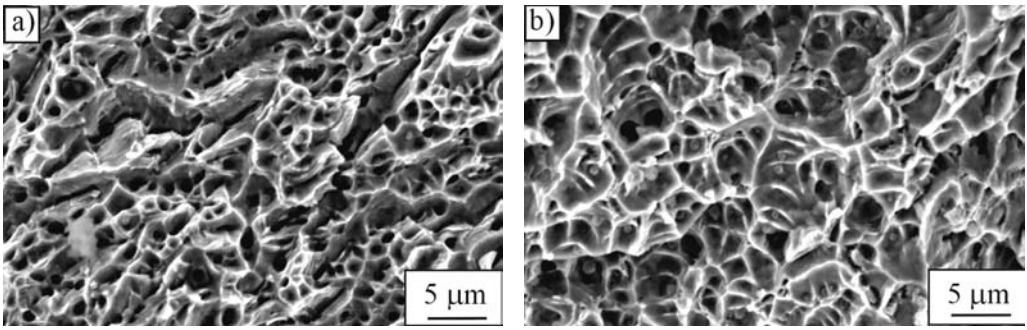

Figure 8. SEM microfractograph of AISI 316L steel weld metal after tensile testing (a) and after Charpy impact testing (b). Specimens annealed at 600 °C.
Slika 8. Mikrofraktografija prelomne površine vara jekla AISI 316L nastale pri nateznem preizkusu (a) in pri epruveti za merjenje udarne žilavosti (b). Epruveti sta bili žarjeni na 600 °C.

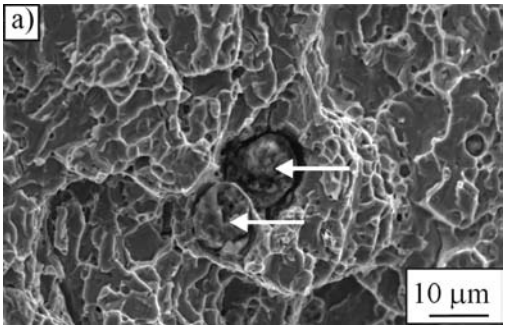

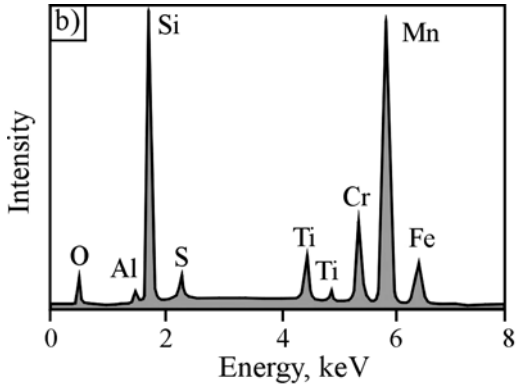

Element	Line	Intensity (c/s)	Concentration (wt.%)
O	K_α	20.49	2.09
Al	K_α	12.34	0.86
Si	K_α	271.44	16.68
S	K_α	21.16	1.18
Ti	K_α	70.80	4.66
Cr	K_α	122.50	11.29
Mn	K_α	534.13	58.54
Fe	K_α	31.19	3.95
Other			0.75

Figure 9. SEM microfractograph of AISI 316L steel weld metal after Charpy impact testing (a) with the corresponding EDX particle spectrum (b). Specimens annealed at 900 °C.
Slika 9. Mikrofraktografija prelomne površine epruvete za preizkus udarne žilavosti vara jekla AISI 316L (a) z mikroanalizo nekovinskega vključka (b). Zvar je bil žarjen na temperaturi 900 °C.

observed, ductile fracture and cleavage fracture. Fracture surfaces of the tensile and impact tested specimens were predominantly ductile with a large number of dimples. The EDX analysis demonstrated the presence of complex Mn-Cr-Si-Ti inclusions in the dimples.

POVZETEK

Vpliv žarjenja na lastnosti osnovnega materiala in vara jekla AISI 316L

Iz raziskave mehanskih lastnosti in mikrostrukture osnovnega materiala in varov jekla AISI 316L po varjenju in po naknadni toplotni obdelavi, lahko povzamemo naslednje:

- Natezna trdnost vara je večja od trdnosti osnovnega materiala. Žilavost in kontrakcija padata skokovito s temperaturo žarjenja.
- Trdote v varu so znatno večje od trdote osnovnega materiala. Primerjave trdot pred in po žarjenju kažejo nesignifikantna nihanja.
- Mikrostruktura osnovnega materiala je iz enakoosnih kristalnih zrn avstenita in trakastih delcev ferita δ (3,4 m.%). V varu je več kot 14 m.% ferita δ kot posledica zaporedja strjevanja s primarnim nastankom ferita med ohlajanjem vara.
- Delež ferita δ se zmanjšuje s temperaturo žarjenja. Delež ferita δ v varu, ki razpade pri žarjenju je od 17,6 m.% pri 600 °C do 96,5 m.% pri 900 °C. Pri osnovnem materialu je ta sprememba od 23,5 m.% na 88,2 m.%.
- Po varjenju je mikrostruktura vara iz avstenita in ferita δ. V varu so tudi nekovinski vključki kompleksne kemične sestave v kateri prevladujejo mangan, silicij, titan in krom.
- Po žarjenju zvarov se na faznih mejah ferit δ - avstenit pojavi faza σ kot rezultat transformacije ferita δ.
- Kemična sestava faze σ je v mejah: 65-67 m.% Fe, 22-26 m.% Cr, 5-7 m.% Ni in okoli 2 m.% Mo. Prisotnost faze σ poslabša udarno žilavost.
- Na prelomih smo opazili dve karakteristični morfološki obliki: duktilni, jamičasti in krhki prelom s cepljenjem. Prelomne površine preizkušancev za natezni preizkus udarne žilavosti so pretežno duktilne s številčnimi jamicami v katerih so kompleksni nekovinski vključki.

References

[1] Lula, R. A. (1986): *Stainless Steel*. American Society for Metals, Metals Park, Ohio.

[2] Lippold, J. C., Kotecki, D. J. (2005): *Welding Metallurgy and Weldability of Stainless Steels*. John Wiley&Sons Inc, New Jersey.

[3] Minami, Y., Kimura, H., Ihara, Y. (1986): Microstructural Changes in Austenitic Stainless Steels During Long-Term Aging. *Materials Science and Technology*.; Vol. 2, No. 8, pp. 795-806.

[4] Heino, S., Knutson-Wedel, E. M., Karlsson, B. (1999): Precipitation Behaviour in Heat Affected Zone of Welded Superaustenitic Stainless Steel. *Materials Science and Technology*.; Vol. 15, No. 1, pp. 101-108.

[5] Zhang, W., Debroy, T., Palmer, T. A., Elmer, J. W. (2005): Modeling of Ferrite Formation in a Duplex Stainless Steel Weld Considering Non-uniform Starting Microstructure. *Acta Materialia*.; Vol. 53, No. 16, pp. 4441-4453.

[6] Angella, G., Wynne, B. P., Rainforth, W. M., Beynon, J. H. (2005): Microstructure Evolution of AISI 316L in Torsion at High Temperature. *Acta Materialia*.; Vol. 53, No. 5, pp. 1263-1275.

[7] Kington, A. V., Noble, F. W. (1995): Formation of σ Phase in Wrought 310 Stainless Steel. *Materials Science and Technology*.; Vol. 11, No. 3, pp. 268-275.

[8] Gojić, M., Markotić, A., Kosec, L. (1999): Duplex Stainless Steels in Oil and Petrochemical Industry. *Nafta*.; Vol. 50, No. 7/8, pp. 241-256.

[9] Gojić, M., Kosec, L., Škraba, P., Pinotić, D. (2003): Mikrostrukturna svojstva dupleks nehrđajućeg čelika nakon zavarivanja. *Proceedings International Conference Joining of Corrosion Resistant Materials*. HDTZ, Opatija, pp. 205-212.

[10] Kožuh, S., Gojić, M. (2006): Mikrostruktura austenitnih i dupleks nehrđajućih čelika nakon zavarivanja. *Zavarivanje*.; Vol. 49, No. 5, pp. 177-185.

[11] Sourmail, T. (2001): Precipitation in Creeep Resistant Austenitic Stainless Steels. *Materials Science and Technology*.; Vol. 17, No. 1, pp. 1-14.

[12] ASTM E-370 E8: Tests Methods for Tension Testing of Metallic Materials. ASTM Committee 1994.

[13] Ohkubo, N., Miyakusu, K., Uematsu, Y., Kimura, H. (1994): Effect of Alloying Elements on the Mechanical Properties of the Stable Austenitic Stainless Steel. *ISIJ International*.; Vol. 34, No. 9, pp. 764-772.

[14] Cui, Y., Lundin, C. D., Hariharan, V. (2006): Mechanical Behavior of Austenitic Stainless Steel Weld Metals with Microfissures. *Journal of Materials Processing Technology*.; Vol. 171, No. 1, pp. 150-155.

[15] Gojić, M. (2003): *Tehnike spajanja i razdvajanja materijala*. Metalurški fakultet, Sveučilište u Zagrebu, Sisak.

[16] Farid, M., Molian, P. A. (2000): High-

Brightness Laser Welding of Thin-Sheet 316 Stainless Steel. *Journal of Materials Science*.; Vol. 35, No. 15, pp. 3817-3826.

[17] Tehovnik, F., Vodopivec, F., Kosec, L., Godec, M. (2006): Hot Ductility of Austenite Stainless Steel with a Solidification Structure. *Materiali in Tehnologije*.; Vol. 40, No. 4, pp. 129-137.

[18] Woo, I., Kikuchi, Y. (2002): Weldability of High Nitrogen Stainless Steel. *ISIJ International*.; Vol. 42, No. 12, pp. 1334-1343.

[19] Boothby, R. M. (1986): Solidification and Transformation Behaviour of Niobium-Stabilized Austenitic Stainless Steel Weld Metal. *Materials Science and Technology*.; Vol. 2, No. 1, pp. 78-87.

[20] San Martin, D., Rivera Diaz del Castillo, P. E. J., Peekstok, E., Van der Zwaag, S. (2007): A New Etching Route for Revealing the Austenite Grain Boundaries in an 11.4% Cr Precipitation Hardening Semi-Austenitic Stainless Steel. *Materials Characterization*.; Vol. 58, No. 5, pp. 455-460.

[21] Padilha, A. F., Rios, P. R. (2002): Decomposition of Austenite in Austenitic Stainless Steels. *ISIJ International*.; Vol. 42, No. 4, pp. 325-337.

[22] David, S. A. (1981): Ferrite Morphology and Variations in Ferrite Content in Austenitic Stainless Steel Welds. *Welding Journal*.; Vol. 60, pp. 63-71.

[23] Park, S. H. C., Sato, Y. S., Kokawa, H., Okamoto, K., Hirano, S., Inagaki, M. (2003): Rapid Formation of the Sigma Phase in 304 Stainless Steel During Friction Stir Welding. *Scripta Materialia*.; Vol. 49, No. 12, pp. 1175-1180.